Status of gyro-Landau-fluid development in BOUT++

C. H. Ma[1, 2]

X. Q. Xu[2], P. W. Xi[1, 2], T. Y. Xia[2,3], T.F. Tang[1,4], A. Dimits[2], M. V. Umansky[2], S. S. Kim[5] , I. Joseph[2], P Snyder[6]

[1]Fusion Simulation Center, School of Physics, Peking University, Beijing, China
[2]Lawrence Livermore National Laboratory, Livermore, CA 94550, USA
[3]Institute of Plasma Physics, Chinese Academy of Sciences, Hefei, China
[4]Dalian University of Technology, Dalian, China
[5]WCI Center for Fusion Theory, NFRI, Korea
[6]General Atomics, San Diego, CA 92186, USA

Presented at 2015 BOUT++ mini-workshop
December 16, 2015 • Livermore, California

LLNL-PRES-680185

Outline

- Introduction
- Code structure
  - Normalization
  - Implementation
  - User interface
- Applications
  - Benchmarks
  - Physics results
- Summary

3+1 GLF simulations in BOUT++

- Turbulent transport constrains the pedestal gradient in the edge;
- The linear KBM physics in EPED[1] successfully predicts the H-mode pedestal height and width;
- 3+1 gyro-Landau-fluid (GLF) model is implemented in BOUT++ to include the KBM turbulence effects in nonlinear ELM simulations.

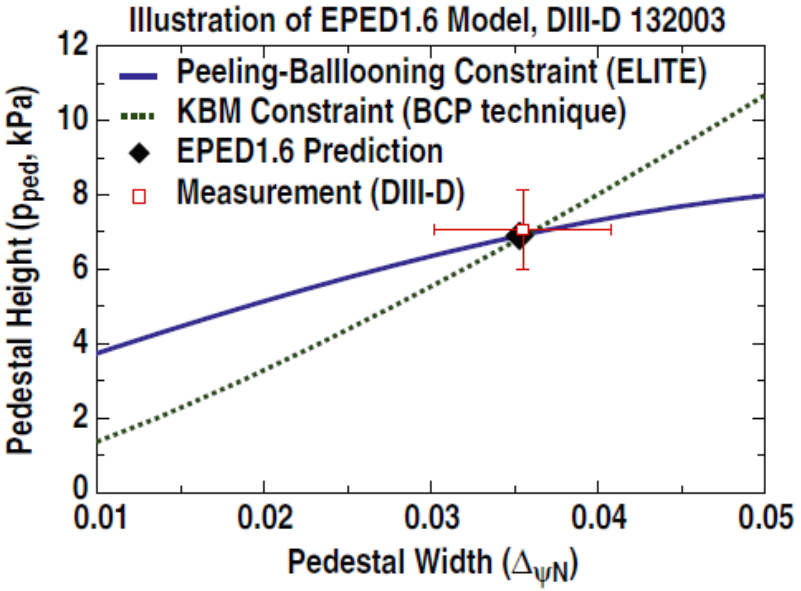

1. P. B. Snyder , et al., NF(2011)

3+1 Gyro-Landau-fluid model

- We utilize the gyrofluid model[1] developed by P. Snyder and G. Hammett;
- 3+1 model: $(n_i, v_{\parallel i}, p_{\parallel i}, p_{\perp i}, \varpi, A_\parallel, p_{\parallel e}, p_{\perp e})$
  - Full FLR effects (Padé approximation): $k_\perp \rho_i \sim 1$;
  - Parallel Landau damping: non-local transport;
    - Non-Fourier methods
    - Both in collisionless[2] and weakly-collisional[3] limits
  - Toroidal resonance;
  - Non-isotropic response ($p_\parallel \neq p_\perp$)
- In long-wavelength limit ($k_\perp \rho_i \ll 1$) and isotropic assumption ($p_\parallel = p_\perp$), the set of equations is reduced to 6-field Landau-fluid model[2] with gyro-viscosity.

1. P. B. Snyder and G. W. Hammett, PoP (2001)
2. A. M. Dimits, *et al.*, PoP (2014)
3. M.V. Umansky, *et al.*, *J. Nucl. Mater.* (2015)
4. T. Y. Xia, X. Q. Xu and P. W. Xi, Nucl. Fusion (2013)

Gyrofluid equations are derived by moments hierarchy from gyrokinetic equations

$f(\boldsymbol{x}, \boldsymbol{v})$

$f(R, v_\parallel, \mu)$

$n(R), u_\parallel(R),$
$p_\parallel(R), p_\perp(R),$
$q_\parallel(R), q_\perp(R),$
...

Kinetic model: 6D

$$\frac{\partial f}{\partial t} + \nabla \cdot \boldsymbol{v} f + \nabla_v \cdot \frac{e}{m}(\boldsymbol{E} + \boldsymbol{v} \times \boldsymbol{B}) f = 0$$

Average over gyro-motion which μ is adiabatically conserved

Gyrokinetic model: 5D

$$\frac{\partial f}{\partial t} + \dot{\boldsymbol{R}} \cdot \nabla f + \dot{v}_\parallel \frac{\partial f}{\partial v_\parallel} = 0$$

moments

Gyrofluid model: 3D

$$n = \int f d^3v \qquad n u_\parallel = \int f v_\parallel d^3v$$
$$p_\parallel = m \int f (v_\parallel - u_\parallel)^2 d^3v$$
$$p_\perp = m \int f B \mu d^3v$$
$$q_\parallel = -3 m v_t^2 n_0 u_\parallel + m \int f v_\parallel^3 \quad d^3v$$
$$q_\perp = -m v_t^2 n_0 u_\parallel + m \int f B \mu v_\parallel d^3v$$

Full set of ion equations in 3+1 GLF model

$$\frac{\partial \tilde{n}_i}{\partial t} = -\frac{1}{B_0} b_0 \times \nabla\Phi \cdot \nabla n_i - \frac{1}{eB_0} b_0 \times \kappa \cdot \nabla (p_{\parallel i} + p_{\perp i})$$

$$- \frac{n_i}{B_0} b_0 \times \kappa \cdot \nabla \left(2 + \frac{1}{2}\hat{\nabla}_\perp^2\right)\Phi - n_0 B_0 \tilde{\nabla}_\parallel \frac{\tilde{u}_{\parallel i}}{B_0} - \frac{n_0}{2T_0 B_0} b_0 \times \nabla \left(\hat{\nabla}_\perp^2 \Phi\right) \cdot \nabla T_{\perp i}$$

$$n_0 \frac{\partial \tilde{u}_{\parallel i}}{\partial t} + n_0 v_\Phi \cdot \nabla \tilde{u}_{\parallel i} + n_0 v_{\Phi_0} \cdot \nabla \tilde{u}_{\parallel i} + \frac{B}{m_i} \tilde{\nabla}_\parallel \frac{\tilde{p}_\parallel}{B}$$

$$+ \left(\frac{\tilde{p}_{\perp i}}{m_i} + \frac{n_0 e}{2m_i} \hat{\nabla}_\perp^2 \Phi\right) \nabla_\parallel \ln B + \frac{1}{T_0} i\omega_d (\tilde{q}_{\parallel i} + \tilde{q}_{\parallel e}) + \frac{4}{T_0} i\omega_d p_{i0} \tilde{u}_{\parallel i} = 0$$

$$\frac{\partial \tilde{p}_{\parallel i}}{\partial t} = -\frac{1}{B_0} b_0 \times \nabla\Phi \cdot \nabla p_{\parallel i} - \frac{n_0}{2B_0} b_0 \times \nabla \left(\hat{\nabla}_\perp^2 \Phi\right) \cdot \nabla T_{\perp i}$$

$$- \frac{p_{\parallel i}}{B_0} b_0 \times \kappa \cdot \nabla \left(4 + \frac{1}{2}\hat{\nabla}_\perp^2\right)\Phi - 3B_0 \tilde{\nabla}_\parallel \frac{p_{i0} \tilde{u}_{\parallel i}}{B_0} - i\omega_d (\tilde{r}_{\parallel,\parallel} + \tilde{r}_{\parallel,\perp}) - B_0 \tilde{\nabla}_\parallel \frac{\tilde{q}_{\parallel i}}{B_0}$$

$$\frac{\partial \tilde{p}_{\perp i}}{\partial t} = -\frac{1}{B_0} b_0 \times \nabla\Phi_2 \cdot \nabla p_{\perp i} - \frac{n_0}{B_0} b_0 \times \left(\hat{\tilde{\nabla}}_\perp^2 \Phi\right) \cdot \nabla T_{\perp i}$$

$$- \frac{p_{\perp i}}{B_0} b_0 \times \kappa \cdot \nabla \left(3 + \frac{3}{2}\hat{\nabla}_\perp^2 + \hat{\tilde{\nabla}}_\perp^2\right)\Phi - B_0^2 \tilde{\nabla}_\parallel \frac{p_{\perp i} \tilde{u}_{\parallel i}}{B_0^2} - i\omega_d (\tilde{r}_{\parallel,\perp} + \tilde{r}_{\perp,\perp}) - B_0^2 \nabla_\parallel \frac{\tilde{q}_{\perp i}}{B_0^2}$$

FLR effect

Continuity

Compression

Landau damping

Toroidal closure

Vorticity formulation is used with full electron response in 3+1 GLF model

$$\frac{\partial A_\parallel}{\partial t} = -\tilde{\nabla}_\parallel \phi + \frac{B_0}{n_0 e}\tilde{\nabla}_\parallel \frac{\tilde{p}_{\parallel e}}{B_0} + \frac{\eta}{\mu_0}\nabla_\perp^2 A_\parallel - \frac{\eta_H}{\mu_0}\nabla_\perp^4 A_\parallel$$

$$\frac{\partial \tilde{T}_e}{\partial t} = -\frac{1}{B_0} b \times \nabla_\perp \phi \cdot \nabla \tilde{T}_e - \frac{2}{3} T_e \left[\left(\frac{2}{B_0} b \times \kappa \right) \cdot \left(\nabla \phi - \frac{1}{e n_{e0}} \nabla \tilde{P}_e - \frac{5}{2e} \nabla \tilde{T}_e \right) + B_0 \nabla_\parallel \left(\frac{\tilde{u}_{\parallel e}}{B_0} \right) \right] + \frac{2}{3 n_{i0}} \nabla_{\parallel 0} q_{\parallel e}$$

FLR effect

Continuity

Compression

Landau damping

Energy flux

Drift Alfven Wave

$$\frac{\partial \tilde{\varpi}_G}{\partial t} = -\frac{1}{B_0} b_0 \times \nabla \phi \cdot \nabla \varpi_G + B_0^2 \tilde{\nabla}_\parallel \frac{\tilde{J}_\parallel}{B_0} + b_0 \times \kappa \cdot \nabla (\tilde{p}_{\parallel i} + \tilde{p}_{\perp i} + \tilde{p}_{\parallel e} + \tilde{p}_{\perp e})$$

$$+ e B_0 b_0 \times \nabla \phi_f \cdot \nabla n_i + \frac{e B_0 n_0}{T_{i0}} b_0 \times \nabla \left(\hat{\nabla}_\perp^2 \Phi \right) \cdot \nabla T_{\perp i} + e B^2 (\delta \bar{\boldsymbol{b}} - \delta \boldsymbol{b}) \cdot \nabla \frac{n_0 u_{\parallel i}}{B_0} + e n_0 b_0 \times \kappa \cdot \nabla \left(2\phi_f + \hat{\nabla}_\perp^2 \Phi \right)$$

Poisson equation: $\varpi_G = eB \left[\bar{n}_i - \tilde{n}_i - n_0 (1 - \Gamma_0) \frac{e\phi}{T_0} + \frac{e\rho_i^2}{T_0} \nabla n_0 \cdot \nabla (\Gamma_0 - \Gamma_1) \phi \right]$

- Have better numerical property than $\tilde{n}_e$ equation

1. P.W. Xi, X.Q. Xu, *et al.*, *Nucl. Fusion* (2013)

Carefully chosen closures are essential to match kinetic effects

Gyro averaging and Padé approximation:

$$\boldsymbol{v}_\Phi = \frac{1}{B}\boldsymbol{b}\times\nabla\Phi$$
$$\boldsymbol{v}_{\bar{A}_\parallel} = \frac{1}{B}\boldsymbol{b}\times\nabla\bar{A}_\parallel$$
$$\left(\Phi, \bar{A}_\parallel\right) = \Gamma_0^{\frac{1}{2}}\left(\phi, A_\parallel\right)$$

$$\begin{cases}\Gamma_0^{\frac{1}{2}}(b) \approx \frac{1}{1+b/2}\\ \Gamma_0(b) \approx \frac{1}{1+b}\\ \Gamma_0 - \Gamma_1 \approx 1\end{cases} \qquad b = -\rho_i^2\nabla_\perp^2$$

Ion Landau closures:

$$\tilde{q}_{\parallel i} = -n_0\sqrt{\frac{8}{\pi}}v_{T_{th}}\frac{ik_\parallel\tilde{T}_{\parallel i}}{\left|k_\parallel\right| + \frac{0.5}{\lambda_i}}$$
$$\tilde{q}_{\perp i} = -n_0\sqrt{\frac{2}{\pi}}v_{T_{th}}\frac{ik_\parallel}{\left|k_\parallel\right| + \frac{0.5}{\lambda_i}}\left(\tilde{T}_{\perp i} + \frac{e}{2}\hat{\nabla}_\perp^2\Phi\right)$$

Electron Landau closures:

$$\tilde{q}_{\parallel e} = -n_0\sqrt{\frac{8}{\pi}}v_{T_{th}}\frac{ik_\parallel\tilde{T}_{\parallel e}}{\left|k_\parallel\right| + \frac{0.5}{\lambda_e}}$$
$$\tilde{q}_{\perp e} = -n_0\sqrt{\frac{2}{\pi}}v_{T_{th}}\frac{ik_\parallel\tilde{T}_{\perp e}}{\left|k_\parallel\right| + \frac{0.5}{\lambda_e}}$$

Toroidal closures:

$$i\omega_d\left(\tilde{r}_{\parallel,\parallel} + \tilde{r}_{\parallel,\perp}\right) = i\omega_d\left(7\tilde{p}_\parallel + \tilde{p}_\perp - 4T_0\tilde{n} - 2i\frac{|\omega_d|}{\omega_d}\left(\nu_1\tilde{T}_\parallel + \nu_2\tilde{T}_\perp\right)\right)$$ Energy flux

$$i\omega_d\left(\tilde{r}_{\parallel,\perp} + \tilde{r}_{\perp,\perp}\right) = i\omega_d\left(\tilde{p}_\parallel + 5\tilde{p}_\perp - 3T_0\tilde{n} - 2i\frac{|\omega_d|}{\omega_d}\left(\nu_3\tilde{T}_\parallel + \nu_4\tilde{T}_\perp\right)\right)$$ Toroidal closure 2 (Imaginary)

$$i\omega_d\left(\tilde{q}_{\parallel i} + \tilde{q}_{\perp i}\right) = 2n_0T_0\nu_5|\omega_d|\tilde{u}_{\parallel i}$$ Toroidal closure 3 (Real)

Outline

- Introduction
- Code structure
  - Normalization
  - Implementation
  - Inputs
- Applications
  - Benchmarks
  - Physics results
- Summary

Initialization (physics_init)

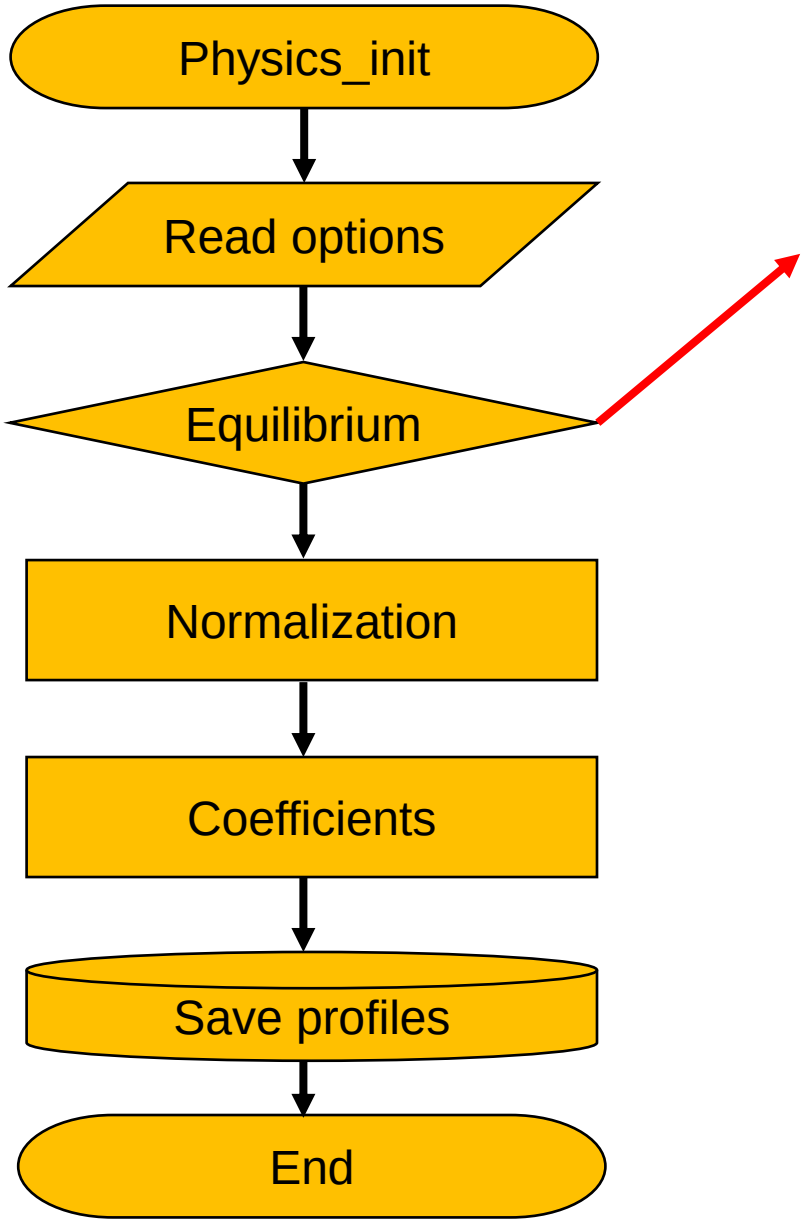

- Equilibrium cases (P0, N0, T0):
  - 1: η_i scan profiles;
  - 2: cyclone case;
  - 4: tanh function profiles;
  - 5: Self-consistent bootstrap current grid;
  - 6: Real geometry with experimental profiles.

Time evolution (physics_run)

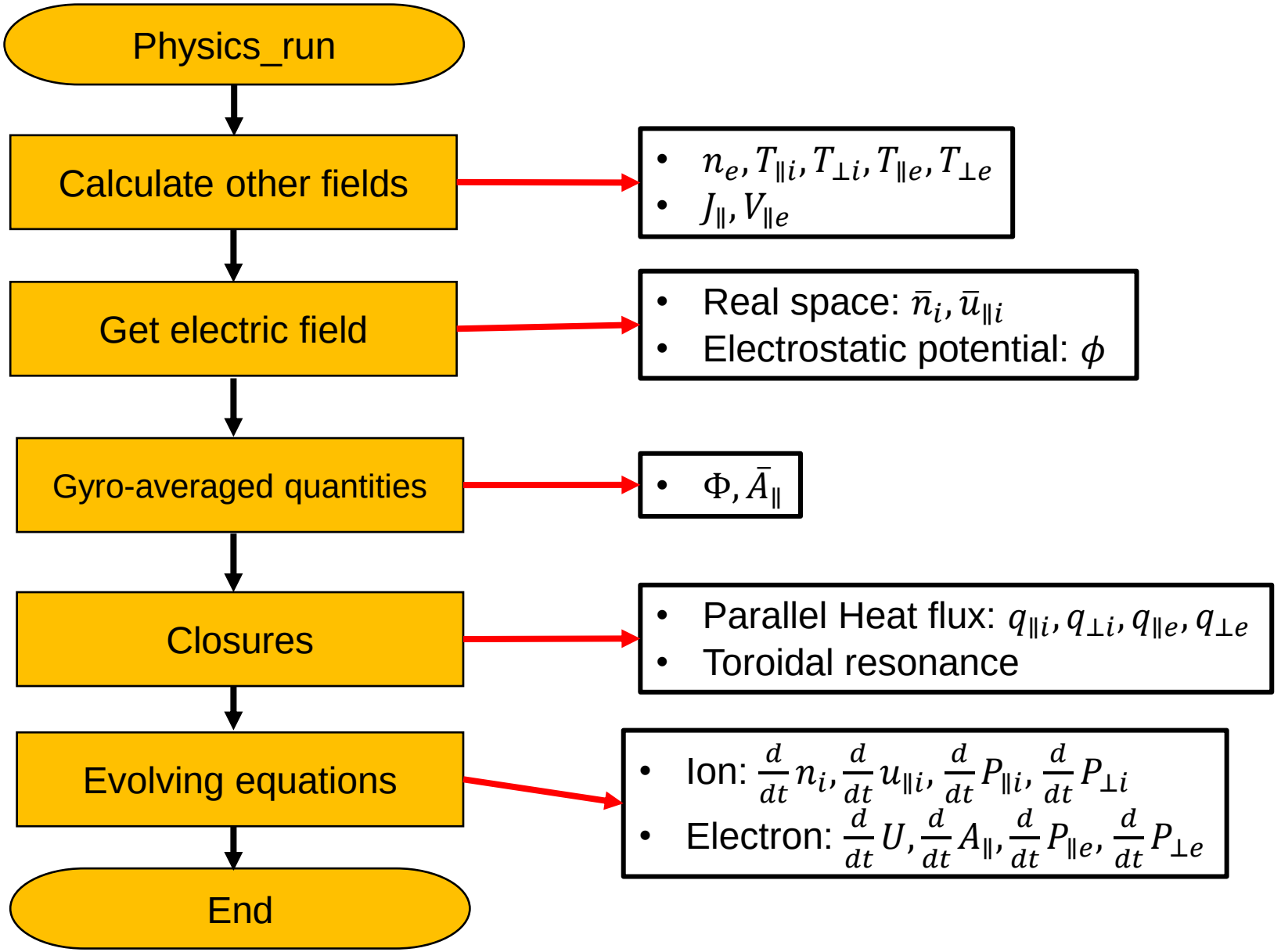

Outline

- Introduction
- Code structure
  - Normalization
  - Implementation
  - Inputs
- Applications
  - Benchmarks
  - Physics results
- Summary

Basic normalized quantities

- Normalization parameters: $(\bar{L}, \bar{T}, \bar{N}, \bar{B})$

$$\bar{V} = \bar{L}/\bar{T}\,, \bar{V}^2 = V_A^2 = \bar{B}^2/\mu_0 m_i \bar{N}\,, \bar{\Omega} = e\bar{B}/m_i\,, C_{nor} = \bar{\Omega}\bar{T}$$

$$\hat{t} = \frac{t}{\bar{T}}, \quad \hat{B} = \frac{B}{\bar{B}}, \quad \hat{\nabla} = \bar{L}\nabla, \quad \hat{\kappa} = \bar{L}\kappa.$$

- Define

$$\psi = A_\parallel/B, \Psi = \bar{A}_\parallel/B, U = \tilde{\varpi}_G/m_i$$

- Evolving variables

$$\hat{n} = \frac{\tilde{n}}{\bar{N}},$$
$$\hat{u}_\parallel = \frac{\tilde{u}_\parallel}{\bar{V}},$$
$$\hat{p} = \frac{\tilde{p}}{m_i \bar{V}^2 \bar{N}},$$
$$\hat{U} = \frac{\bar{T}}{\bar{N}} U,$$
$$\hat{\psi} = \frac{\psi}{\bar{L}}.$$

other important variables

$$\hat{T} = \frac{\tilde{T}}{m_i \bar{V}^2},$$
$$\hat{\eta} = \frac{\bar{T}}{\bar{L}^2 \mu_0} \eta,$$
$$\hat{J}_{\parallel c} = \bar{L} J_{\parallel c},$$
$$\hat{\varpi}_G = \frac{\varpi_G}{e\bar{B}\bar{N}},$$
$$\hat{\phi} = \frac{\phi}{\bar{L}\bar{V}\bar{B}}.$$

Normalized ion equations

$$\frac{\partial \hat{n}_i}{\partial \hat{t}} = -[\hat{\Phi}, \hat{n}_{G0}] - [\hat{\Phi}_0, \hat{n}_{G0}] - [\hat{\Phi}, \hat{n}_i] - \frac{1}{C_{nor}\hat{B}_0} b_0 \times \hat{\kappa} \cdot \hat{\nabla}(\hat{p}_{\parallel i} + \hat{p}_{\perp i})$$
$$- \frac{\hat{n}_0}{\hat{B}_0} b_0 \times \hat{\kappa} \cdot \hat{\nabla} \left(2 + \frac{1}{2}\hat{\nabla}_\perp^2\right) \hat{\Phi} - \frac{\hat{n}_i}{\hat{B}_0} b_0 \times \hat{\kappa} \cdot \hat{\nabla} \left(2 + \frac{1}{2}\hat{\nabla}_\perp^2\right) \hat{\Phi}$$
$$- \hat{n}_0 \hat{B}_0 \hat{\nabla}_\parallel \frac{\hat{u}_{\parallel i}}{\hat{B}_0} - \hat{n}_i \hat{B}_0 \hat{\nabla}_\parallel \frac{\hat{u}_{\parallel i}}{\hat{B}_0} - \frac{\hat{n}_0}{2\hat{T}_0} [\hat{\nabla}_\perp^2 \hat{\Phi}, \hat{T}_{i0}] - \frac{1}{2} \left[\hat{\nabla}_\perp^2 \hat{\Phi}, \frac{\hat{n}_0 \hat{T}_{\perp i}}{\hat{T}_{i0}}\right]$$

$$\frac{\partial \hat{u}_{\parallel i}}{\partial \hat{t}} = -[\hat{\Phi}, \hat{u}_{\parallel i}] - \frac{1}{\tilde{n}_0} \tilde{\nabla}_\parallel \hat{p}_\parallel + \frac{\hat{B}_0}{\hat{n}_0} [\hat{\psi}, \hat{P}_0]$$
$$- \frac{4}{C_{nor}\hat{B}_0} b_0 \times \hat{\kappa} \cdot \hat{\nabla} \hat{T}_{i0} \hat{u}_{\parallel i} - \frac{\hat{p}_{\perp i}}{\hat{n}_0 \hat{B}_0} \nabla_{\parallel 0} B_0 - \frac{C_{nor}}{B_0} \hat{\nabla}_\perp^2 \hat{\Phi} \hat{\nabla}_{\parallel 0} B - \frac{1}{\hat{p}_{i0}} i\omega_d (\hat{q}_{\parallel i} + \hat{q}_{\perp i})$$

$$\frac{\partial \hat{p}_{\parallel i}}{\partial \hat{t}} = -[\hat{\Phi}, \hat{p}_{i0}] - [\hat{\Phi}, \hat{p}_{\parallel i}] - \frac{\hat{n}_0}{2} [\hat{\nabla}_\perp^2 \Phi, \hat{T}_{i0}] - \frac{\hat{n}_0}{2} [\hat{\nabla}_\perp^2 \hat{\Phi}, \hat{T}_{\perp i}]$$
$$- \frac{\hat{p}_{i0}}{\hat{B}_0} b_0 \times \hat{\kappa} \cdot \hat{\nabla} \left(4 + \frac{1}{2}\hat{\nabla}_\perp^2\right) \hat{\Phi} - \frac{\hat{p}_{\parallel i}}{\hat{B}_0} b_0 \times \hat{\kappa} \cdot \hat{\nabla} \left(4 + \frac{1}{2}\hat{\nabla}_\perp^2\right) \hat{\Phi}$$
$$- 3\hat{B}_0 \hat{\nabla}_\parallel \frac{\hat{p}_{i0} \hat{u}_{\parallel i}}{\hat{B}_0} - 3\hat{B}_0 \hat{\nabla}_{\parallel 0} \frac{\hat{p}_{\parallel i} \hat{u}_{\parallel i}}{\hat{B}_0} - i\omega_d (\hat{r}_{\parallel,\parallel} + \hat{r}_{\parallel,\perp}) - \hat{B}_0 \hat{\nabla}_\parallel \frac{\hat{q}_{\parallel i}}{\hat{B}_0}$$

$$\frac{\partial p_{\perp i}}{\partial \hat{t}} = -[\hat{\Phi}_2, \hat{p}_{i0}] - [\hat{\Phi}_2, \hat{p}_{\parallel i}] - \hat{n}_0 [\hat{\hat{\nabla}}_\perp^2 \hat{\Phi}, \hat{T}_{i0}] - \hat{n}_0 [\hat{\hat{\nabla}}_\perp^2 \hat{\Phi}, \hat{T}_{\perp i}]$$
$$- \frac{\hat{p}_{i0}}{\hat{B}_0} b_0 \times \hat{\kappa} \cdot \hat{\nabla} \left(3 + \frac{3}{2}\hat{\nabla}_\perp^2 + \hat{\hat{\nabla}}_\perp^2\right) \hat{\Phi} - \frac{\hat{p}_{\perp i}}{\hat{B}_0} b_0 \times \hat{\kappa} \cdot \hat{\nabla} \left(3 + \frac{3}{2}\hat{\nabla}_\perp^2 + \hat{\hat{\nabla}}_\perp^2\right) \hat{\Phi}$$
$$- \hat{B}_0^2 \hat{\nabla}_\parallel \frac{\hat{p}_{i0} \hat{u}_{\parallel i}}{\hat{B}_0^2} - \hat{B}_0^2 \hat{\nabla}_{\parallel 0} \frac{\hat{p}_{\perp i} \hat{u}_{\parallel i}}{B_0^2} - i\omega_d (\hat{r}_{\parallel,\perp} + \hat{r}_{\perp,\perp}) - \hat{B}_0^2 \hat{\nabla}_{\parallel 0} \frac{\hat{q}_{\perp i}}{\hat{B}_0^2}$$

Normalized electron equations

$$\frac{\partial \hat{\psi}}{\partial \hat{t}} = -\frac{1}{\hat{B}_0}\hat{\nabla}_{\parallel}\hat{\phi} + \frac{1}{C_{nor}\hat{n}_0\hat{B}_0}\hat{\nabla}_{\parallel}\hat{p}_{\parallel e} + \frac{1}{C_{nor}\hat{n}_0}[\hat{\psi}, \hat{P}_{e0}] + \hat{\eta}\hat{J}_{\parallel c} - \hat{\eta}_H\hat{\nabla}_{\perp}^2\hat{J}_{\parallel c}$$

$$\frac{\partial \hat{T}_e}{\partial t} = -[\hat{\phi}, \hat{T}_{e0} + \hat{T}_e] - \frac{2}{3}\left(\hat{T}_{e0} + \hat{T}_e\right)\left[\hat{B}_0\hat{\nabla}_{\parallel}\left(\frac{\hat{u}_{\parallel e}}{\hat{B}_0}\right) + \left(\frac{2}{\hat{B}_0}b \times \hat{\kappa}\right)\cdot\left(\hat{\nabla}\hat{\phi} - \frac{1}{\hat{n}_{e0}C_{nor}}\nabla\hat{p}_e - \frac{5}{2C_{nor}}\nabla\hat{T}_e\right)\right] + \frac{2}{3\hat{n}_{i0}}\hat{\nabla}_{\parallel 0}\hat{q}_{\parallel e}$$

Normalized vorticity equations

$$\frac{\partial \hat{U}}{\partial \hat{t}} = -[\hat{\phi}, \hat{U}_0] - [\hat{\phi}, \hat{U}] - \frac{V_A^2}{\bar{V}^2}\hat{B}_0^2 \hat{\nabla}_\parallel \hat{J}_{\parallel c} - \hat{B}_0^3[\hat{\psi}, \hat{J}_0] + b_0 \times \hat{\kappa} \cdot \hat{\nabla}(\hat{p}_{\parallel i} + \hat{p}_{\perp i} + \hat{p}_{\parallel e} + \hat{p}_{\perp e})$$

$$+ C_{nor}\hat{B}_0[\hat{\phi}_f, \hat{n}_0] + C_{nor}\hat{B}_0[\hat{\phi}_f, \hat{n}_i] + \frac{C_{nor}\hat{B}_0\hat{n}_0}{\hat{T}_{i0}}[\hat{\nabla}_\perp^2 \hat{\Phi}, \hat{T}_{i0}] + \frac{C_{nor}\hat{B}_0\hat{n}_0}{\hat{T}_{i0}}[\hat{\nabla}_\perp^2 \hat{\Phi}, \hat{T}_{\perp i}]$$

$$- C_{nor}\hat{B}_0^3 \left[\hat{\Psi} - \hat{\psi}, \frac{\hat{n}_0 \hat{u}_{\parallel i}}{\hat{B}_0}\right] + C_{nor}\hat{n}_0 b_0 \times \hat{\kappa} \cdot \hat{\nabla}\left(2\hat{\phi}_f + \hat{\nabla}_\perp^2 \hat{\Phi}\right)$$

Where:

$$U = \frac{\varpi_G}{m_i} \qquad \hat{\varpi}_G = \hat{B}(\hat{n}_e - \hat{n}_i), \qquad \hat{U} = C_{nor}\hat{\varpi}_G.$$

Outline

- Introduction
- Code structure
  - Normalization
  - Implementation
  - Inputs
- Applications
  - Benchmarks
  - Physics results
- Summary

Gyro-average operator

- Gyro-average operator with Pade approximation:

$$\boldsymbol{v}_{\Phi} = \frac{1}{B}\boldsymbol{b} \times \nabla\Phi$$

$$\boldsymbol{v}_{\bar{A}_{\parallel}} = \frac{1}{B}\boldsymbol{b} \times \nabla\bar{A}_{\parallel}$$

$$\left(\Phi, \bar{A}_{\parallel}\right) = \Gamma_0^{\frac{1}{2}}\left(\phi, A_{\parallel}\right)$$

$$\begin{cases} \Gamma_0^{\frac{1}{2}}(b) \approx \frac{1}{1+b/2} \\ \Gamma_0(b) \approx \frac{1}{1+b} \\ \Gamma_0 - \Gamma_1 \approx 1 \end{cases} \qquad b = -\rho_i^2\nabla_{\perp}^2$$

- Multiply the denominator in the operator:

$$\left(1 - \rho_i^2\nabla_{\perp}^2\right)\Phi = \phi$$

- This equation is solved using Laplacian inversion in the code:

```
gyrophi = invert_laplace(phi,phi_flags,&gyroa,NULL,&gyrob);
```

Modified Laplacian operators

- The modified Laplacian operators can be expressed as the subtract of gyro-average operators:

$$\begin{aligned}\hat{\nabla}_\perp^2\Phi =& 2b\frac{\partial\Gamma_0^{\frac{1}{2}}}{\partial b}\phi \\ =& -\frac{b}{\left(1+\frac{b}{2}\right)^2}\phi \\ =& 2\left[\frac{1}{\left(1+\frac{b}{2}\right)^2}-\frac{1}{1+\frac{b}{2}}\right]\phi \\ =& 2\left[\Phi_2-\Phi\right],\end{aligned}$$

$$\begin{aligned}\hat{\hat{\nabla}}_\perp^2\Phi =& b\frac{\partial^2}{\partial b^2}\left(b\Gamma_0^{\frac{1}{2}}\right)\phi \\ =& -\frac{b}{\left(1+\frac{b}{2}\right)^3}\phi \\ =& 2\left[\frac{1}{\left(1+\frac{b}{2}\right)^3}-\frac{1}{\left(1+\frac{b}{2}\right)^2}\right]\phi \\ =& 2\left[\Phi_3-\Phi_2\right],\end{aligned}$$

where $\Phi_2=\Gamma_0^{\frac{1}{2}}\Phi$ and $\Phi_3=\Gamma_0^{\frac{1}{2}}\Phi_2$.

Poisson equation

- The gyro-kinetic Poisson equation is

$$U = \frac{eB}{m_i}\left[\bar{n}_i - \tilde{n}_i - n_0\left(1-\Gamma_0\right)\frac{e\phi}{T_0} + \frac{e\rho_i^2}{T_0}\nabla n_0 \cdot \nabla(\Gamma_0 - \Gamma_1)\phi\right]$$

- Define

$$\hat{n}_{mid} = \frac{\hat{T}_0}{C_{nor}\hat{n}_0}\left(\hat{\bar{n}}_i - \hat{n}_i - \frac{\hat{U}}{C_{nor}\hat{B}_0}\right)$$

- Poisson equation becomes

$$\left(1-\Gamma_0\right)\hat{\phi} - \frac{\hat{\rho}_i^2}{\hat{n}_0}\hat{\nabla}\hat{n}_0 \cdot \hat{\nabla}(\Gamma_0 - \Gamma_1)\hat{\phi} = \hat{n}_{mid}.$$

- With Pade approximation

$$\hat{\nabla}_\perp^2\hat{\phi} + \frac{1}{\hat{n}_0}\hat{\nabla}\hat{n}_0 \cdot \hat{\nabla}\hat{\phi} = -\frac{1}{\hat{\rho}_i^2}\hat{n}_{mid} + \hat{\nabla}_\perp^2\hat{n}_{mid}$$

- In the code

```
phi = invert_laplace(gyrosour, phi_flags, NULL, &n0, NULL);
```

Poisson equation with adiabatic response

- The adiabatic response is used in the electrostatic simulations;
- The gyro-kinetic Poisson equation with adiabatic response is

$$\frac{n_0\tilde{\phi}}{T_{e0}} + \frac{n_0}{T_{i0}}(1-\Gamma_0)\tilde{\phi} = \Gamma_0^{1/2}\tilde{n}_i + \frac{n_0}{T_{i0}} b \frac{\partial \Gamma_0^{1/2}}{\partial b}\tilde{T}_{i\perp}$$

- After normalization and Pade approximation, the equation becomes

$$-2\hat{\rho}_i \nabla_\perp^2 \hat{\phi} + \hat{\phi} = (1-\hat{\rho}_i\nabla_\perp^2)\frac{\hat{T}_0 \bar{n}_i}{C_{nor}\hat{n}_0}$$

- In the code

```
phi = invert_laplace(gyrosour, phi_flags, &phia, NULL, &phid);
```

Outline

- Introduction
- Code structure
  - Normalization
  - Implementation
  - Inputs
- Applications
  - Benchmarks
  - Physics results
- Summary

Options in the input file

Option	Description
electrostatic	Solve Poisson equation with adiabatic response, instead of solving the electron equations.
eHall	Electron drift wave terms
Gyroaverage	Gyro-average and FLR effect terms
FLR_effect	
Continuity	Compressible terms
Compression	Parallel viscosity
Isotropic (default: false)	Average the parallel and perpendicular pressure
Landau_damping_i	Landau damping terms for ions
Landau_damping_wcoll_i	Collisional terms in ion Landau damping
Landau_damping_e	Landau damping terms for electrons
Landau_damping_wcoll_e	Collisional terms in electron Landau damping
Energy_flux	Energy flux terms in toroidal closures
Toroidal_closure2	The imaginary part of $\|\omega_d\|$ terms in toroidal closures
Toroidal_closure3	The real part of $\|\omega_d\|$ terms in toroidal closures

Options in the input file cont.

- curv_model: Controls the implementation of curvature term ($i\omega_d$)
  - 1: $i\omega_d = \frac{T_0}{eB} b \times \kappa \cdot \nabla$;
  - 2: $i\omega_d = \frac{T_0}{eB^2} b \times \nabla B \cdot \nabla$;
  - 3: $i\omega_d = \frac{T_0}{2eB}\left(b \times \kappa \cdot \nabla + \frac{1}{\mathrm{B}} b \times \nabla B \cdot \nabla\right)$;
  - 4: $i\omega_d = \frac{T_0}{eB} b \times \kappa' \cdot \nabla$, where $\kappa' = \frac{\boldsymbol{B}}{B^3} \times \nabla\left(\mu_0 P_0 + \frac{B^2}{2}\right)$ is the magnetic curvature calculated in the code;
  - 5: $i\omega_d = \frac{T_0}{2eB}\left(b \times \kappa' \cdot \nabla + \frac{1}{\mathrm{B}} b \times \nabla B \cdot \nabla\right)$.

Outline

- Introduction
- Code structure
  - Normalization
  - Implementation
  - Inputs
- Applications
  - Benchmarks
  - Physics results
- Summary

Our 3+1 GLF code is benchmarked with other gyro-kinetic and gyro-fluid code in ES ITG simulations

- With adiabatic electron response, the 3+1 GLF results are in good agreement with other gyrofluid code (GLF 3+0) and gyorokinetic code (FULL).

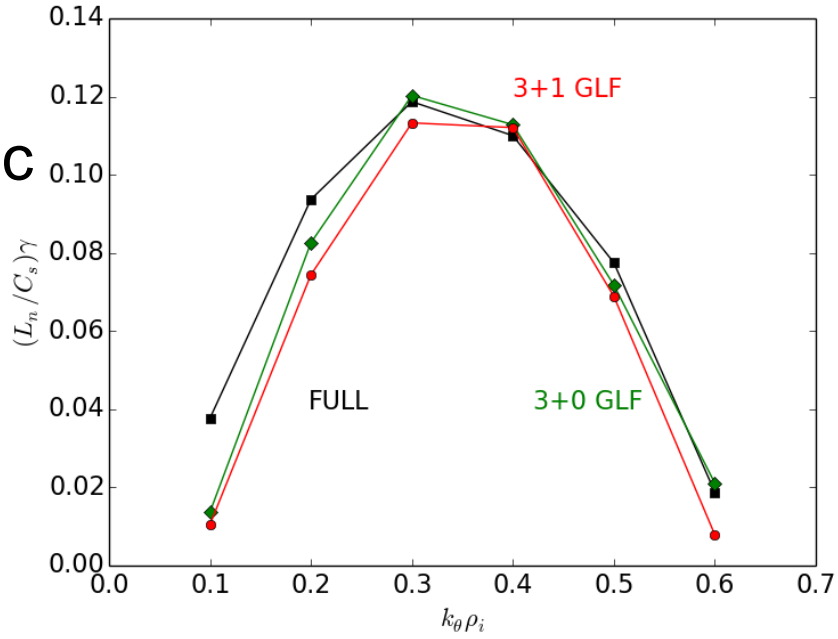

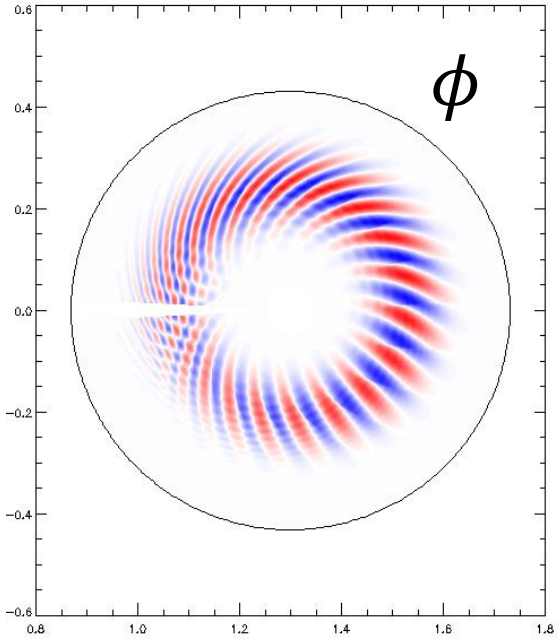

1. C.H. Ma, X.Q. Xu, *et al.*, *PoP* (2015)

Adiabatic response:

$$\frac{n_0\tilde{\phi}}{T_{e0}} + \frac{n_0\tilde{\phi}}{T_{i0}}(1-\Gamma_0)\tilde{\phi} = \Gamma_0^{1/2}\tilde{n}_i + \frac{n_0}{T_{i0}}\, b\, \frac{\partial \Gamma_0^{1/2}}{\partial b}\tilde{T}_{i\perp}$$

The Landau closure with collisions has implemented and tested in BOUT

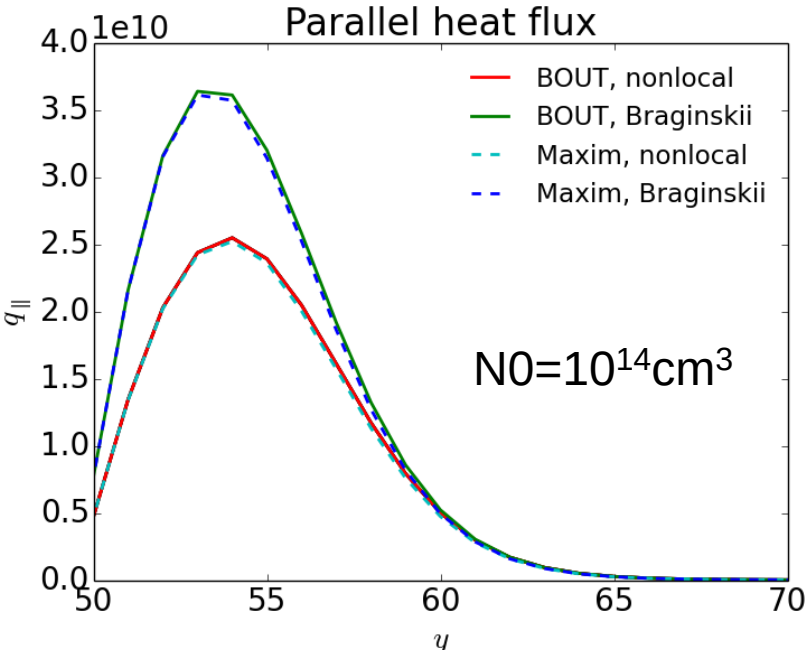

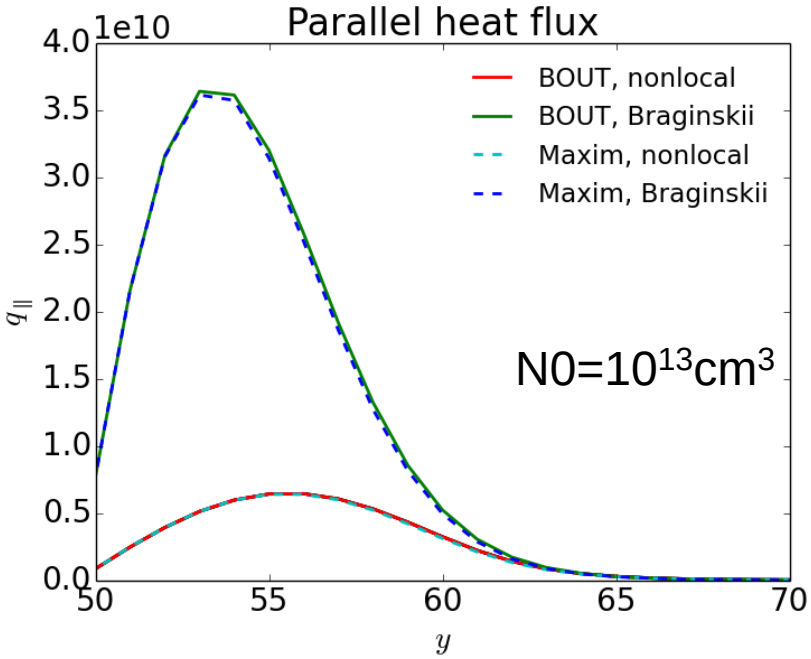

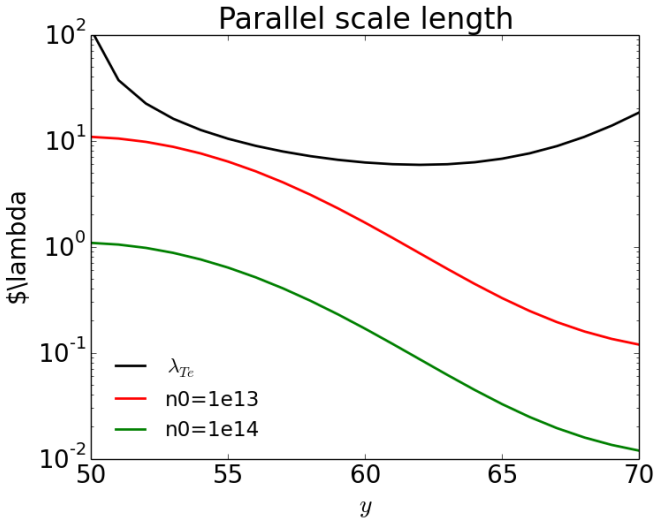

- The nonlocal heat flux has closer results for the stronger collision case;
- The implementation in BOUT++ is well benchmarked with Maxim's results[1].

1. M.V. Umansky, *et al.*, *J. Nucl. Mater.* (2015)

The linear growth rates of 3+1 and 6-field model agree well in lower mode numbers

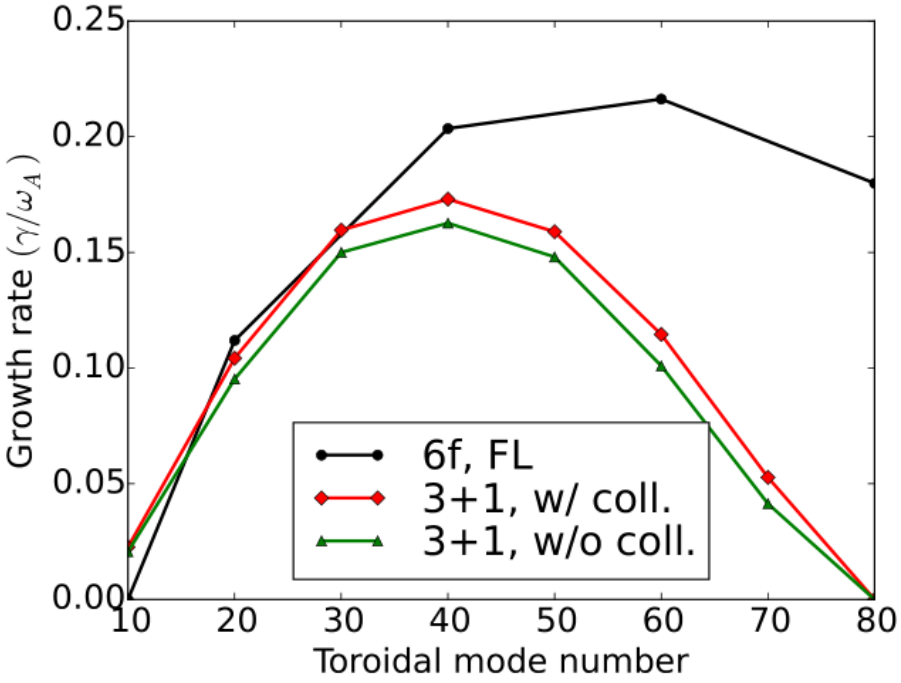

The black curve for 6-field, with the free streaming limitation; The red curve for 3+1 model, with Landau damping and collisions; The blue curve for 3+1 model, with Landau damping, without collision effect.

- The linear growth rate for 6-field model is much larger than the results from 3+1 model, because the diamagnetic effect may not be a good approximation of the FLR effect when $k_\perp \rho_i$ is large;
- The collision effect destabilizes the modes by reducing the parallel heat flux;
- The linear growth rates of 6-field and 3+1 have good agreements in lower mode numbers where $k_\perp \rho_i \ll 1$.

Outline

- Introduction
- Code structure
  - Normalization
  - Implementation
  - Inputs
- Applications
  - Benchmarks
  - Physics results
- Summary

The global beta-scan with a series of self-consistent equilibrium

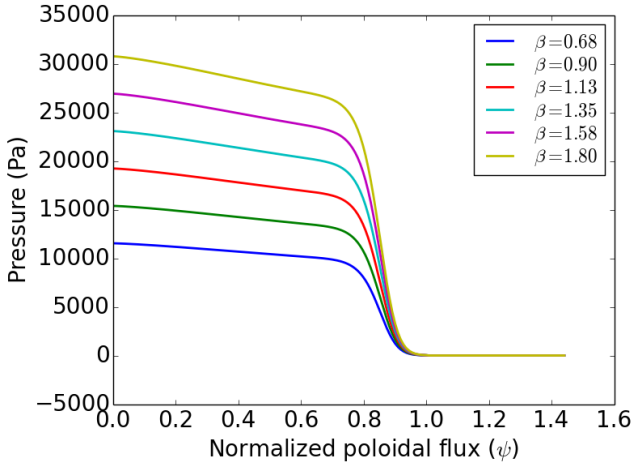

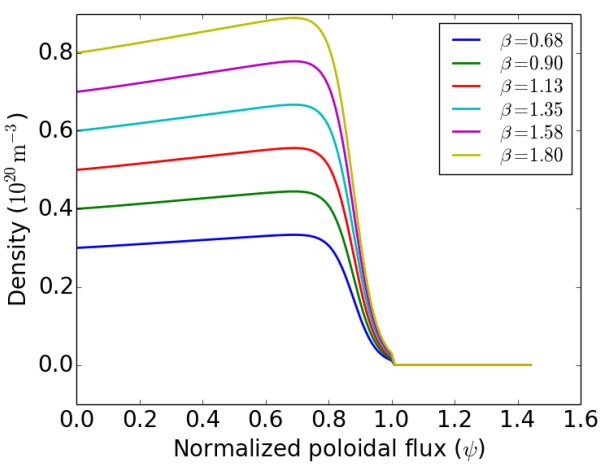

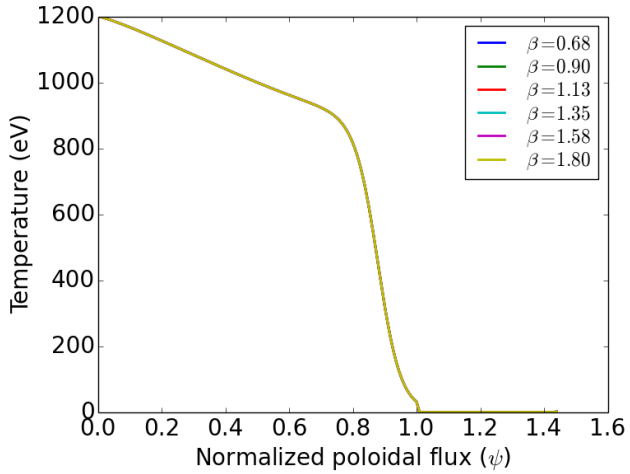

- Jet like equilibrium;
- The temperature profile is fixed;
- The density and pressure profiles increase when β increases.
- Weakly-collisional case, $\nu_e^* < 0.1$
- $\eta_i = 0.685$, the same for all cases.

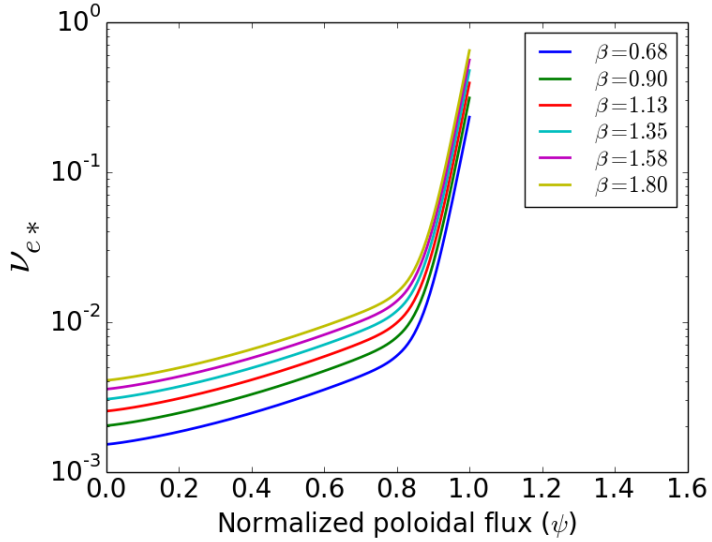

Kinetic physics has stabilizing effects on ballooning modes

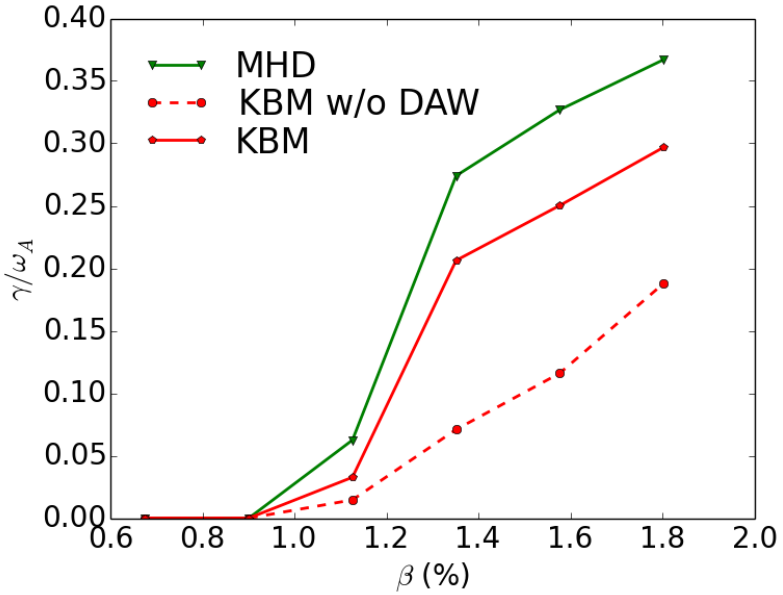

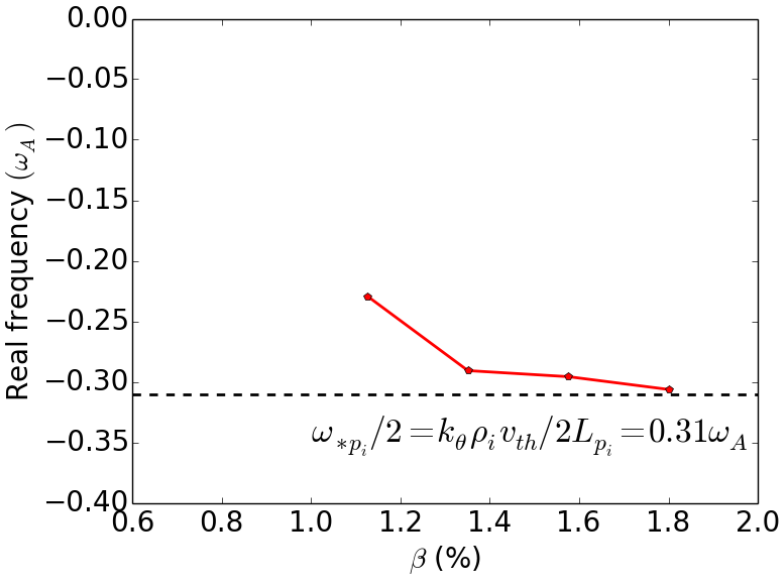

- This is kinetic ballooning modes (KBM) because there is no instability without curvature drive;
- The real frequency is around the theoretical prediction;
- Since $\eta_i < 1$, threshold of KBM and IBM is about the same.

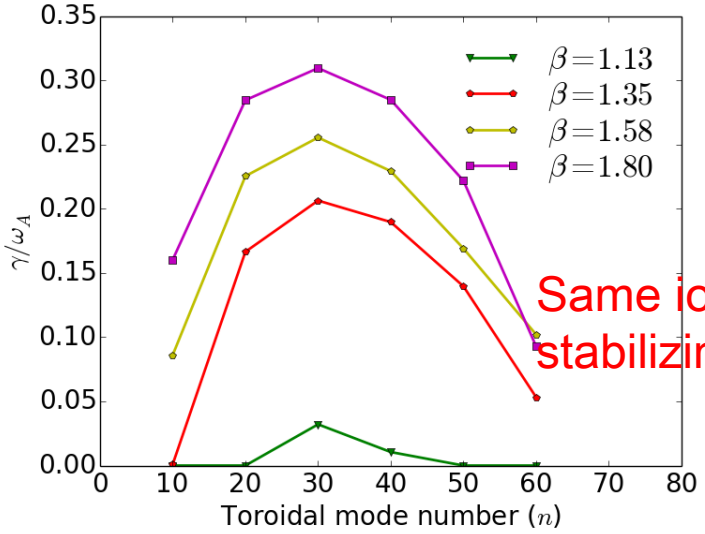

Same ion diamagnetic stabilizing effects!

1. C.H. Ma, X.Q. Xu, *et al.*, *PoP* (2015)

The relative energy loss increases with increasing beta

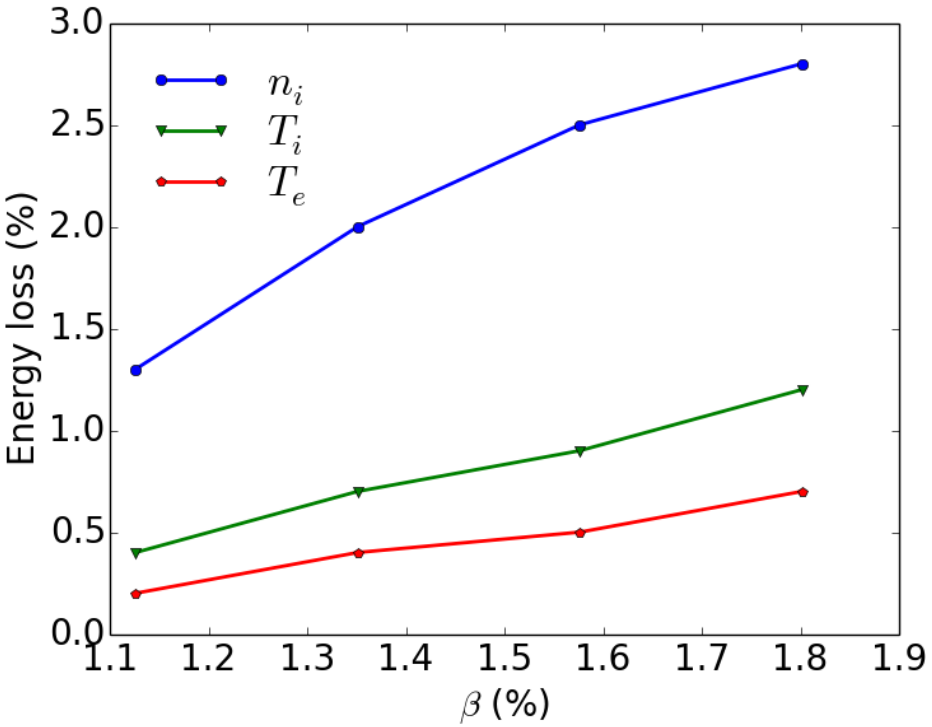

- When beta increases, the relative energy loss of initial crash from all channels increase;
- Convective energy loss is dominant because of the large density height;
- Energy loss from ion is larger than the loss from electron;
- Electron perturbation is damped by the Landau damping effect, which is larger than ions by a factor of $\sqrt{m_i/m_e}$.

KBM is unstable below IBM threshold when temperature gradient is large

- Concentric circular magnetic surfaces without shift;
- The unstable threshold are the same for the constant temperature case ($\eta_i = 0$).;
- The KBM is unstable under ideal ballooning mode threshold when $\eta_i = 2$.
- There is no second stable region in these cases because the Shafranov shift effects is missed;

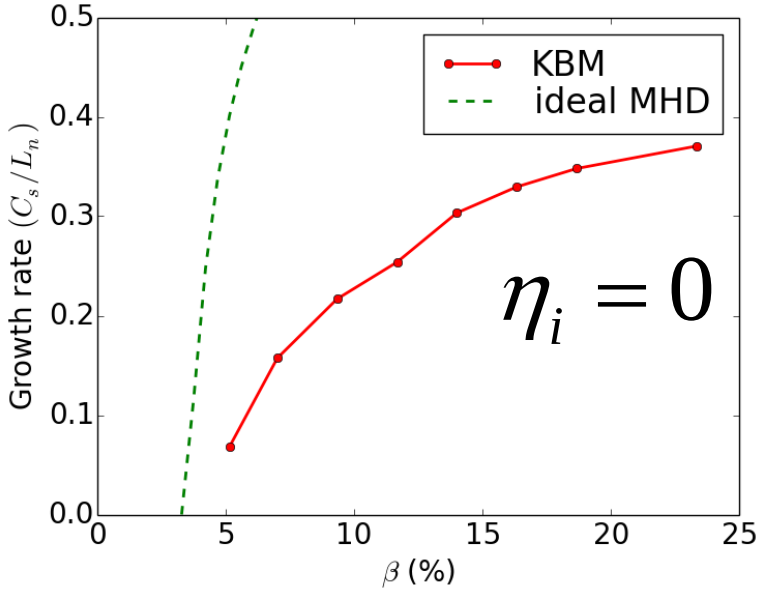

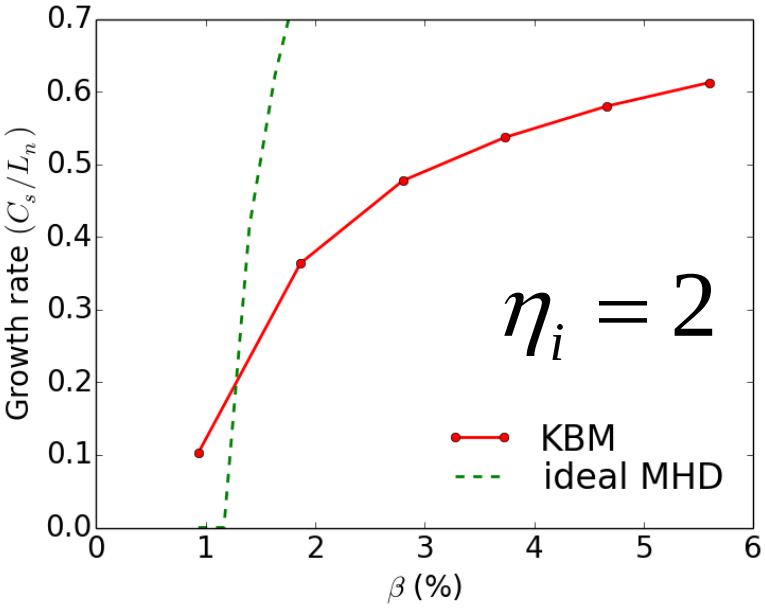

The shift increases with beta in our equilibrium

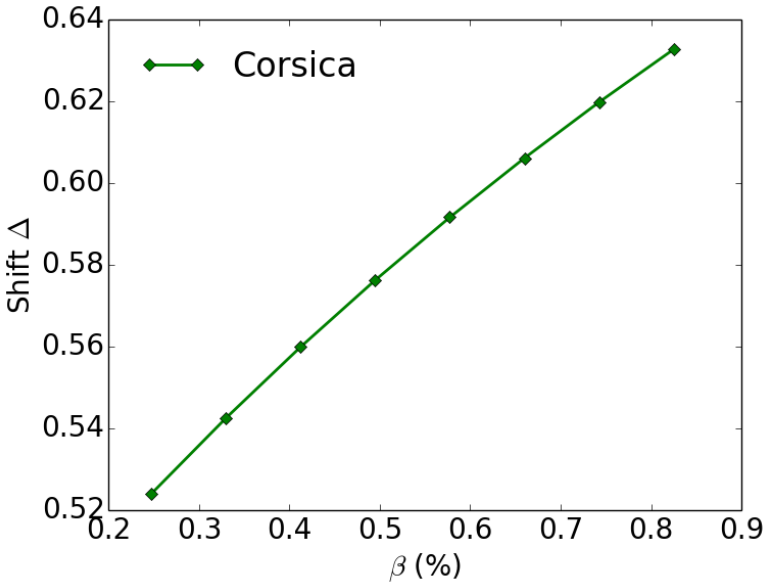

- The shift and maximum elongation increase with beta in the equilibrium.

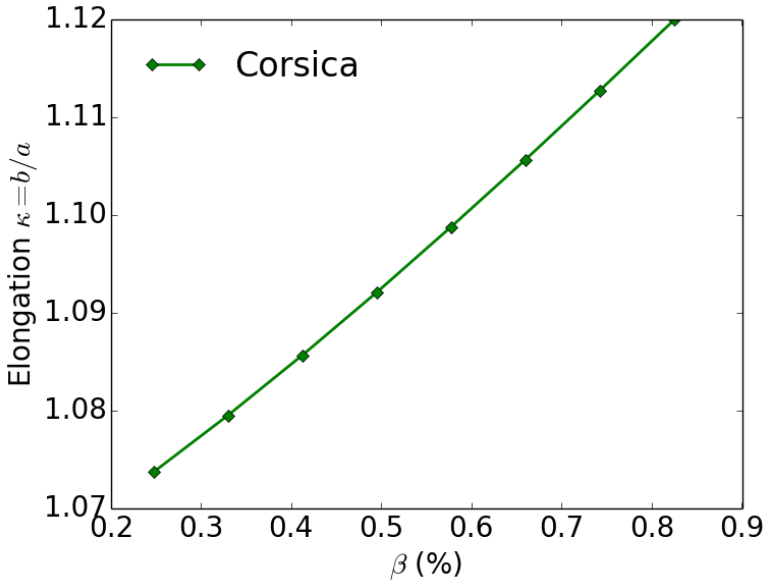

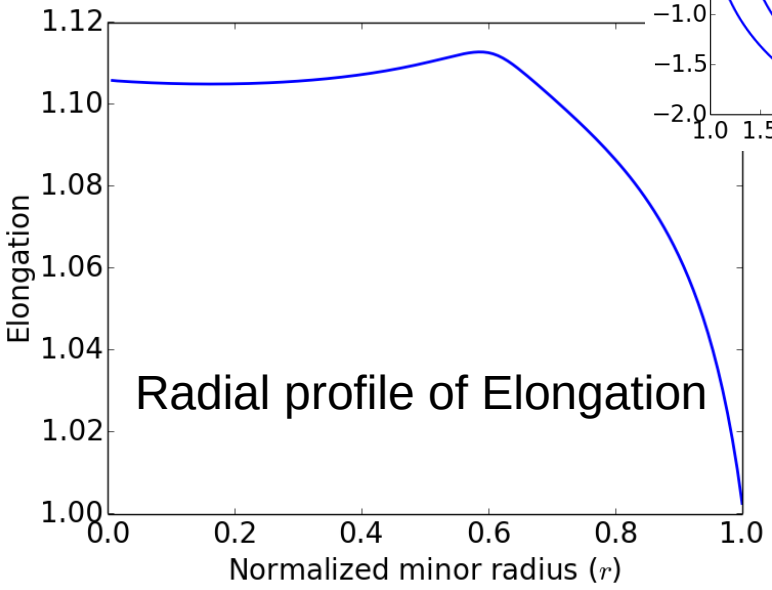

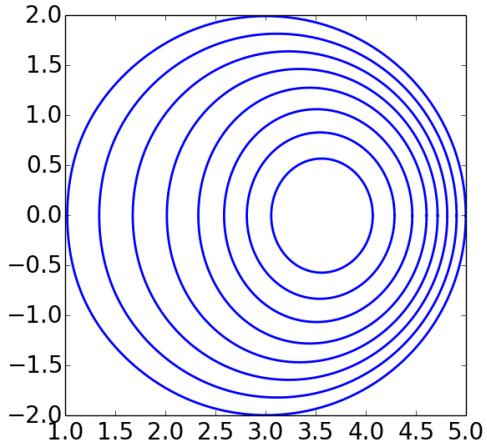

Second stable region of KBM is found in the self consistent beta scan

- Beta scan in a series of self-consistent grids;
- The linear growth rate for the ballooning mode peaks at $\beta = 0.66\%$;
- The KBM is unstable when $\beta_c = 0.4\%$ and $\alpha_c = 1.8$;
- The second stable region of KBM is observed when $\beta > 0.9\%$ and $\alpha > 3.75$;
- The growth rate of ideal ballooning mode is larger than KBM in this case.

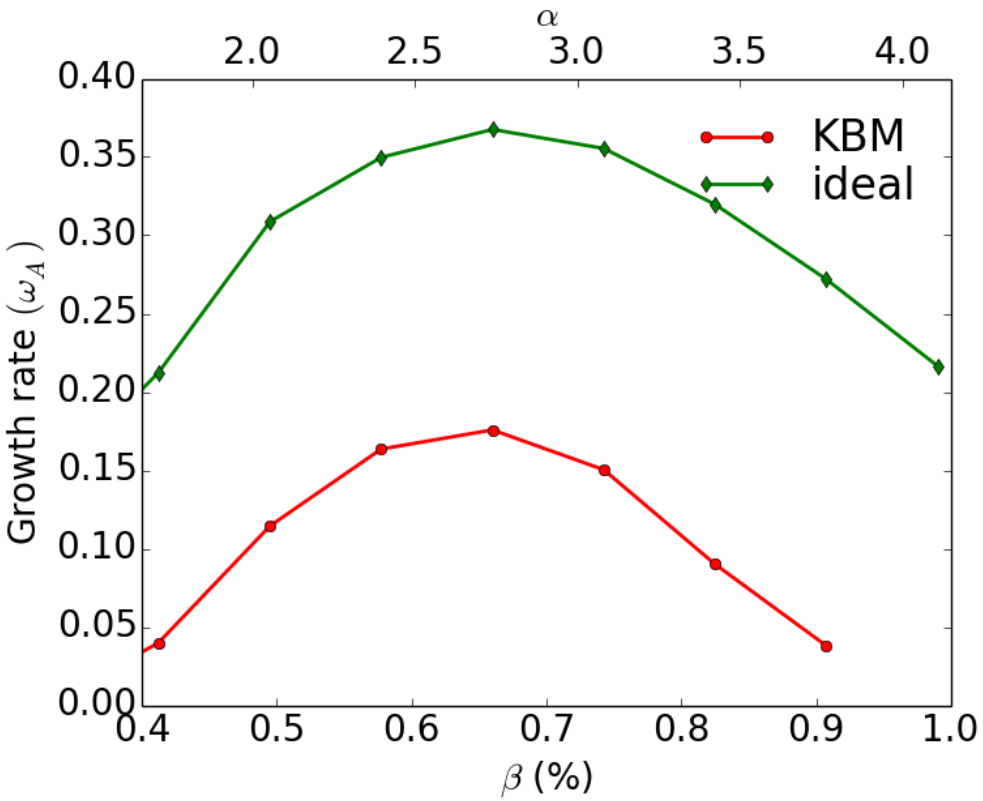

Parameters:

$$n = 20, (k_\theta \rho_i = 0.11)$$
$$q = 2.0, s = 2.70$$
$$R = 3m, a = 2m$$
$$\epsilon_n = 1/18.6, \eta_i = \eta_e = 3.1$$

Initial GLF simulations in X-point geometry

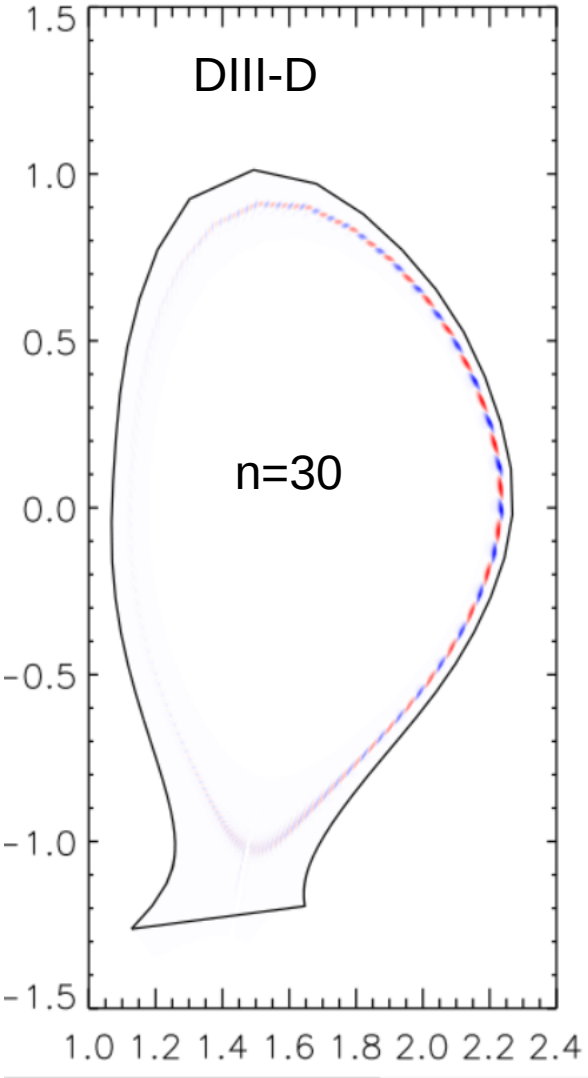

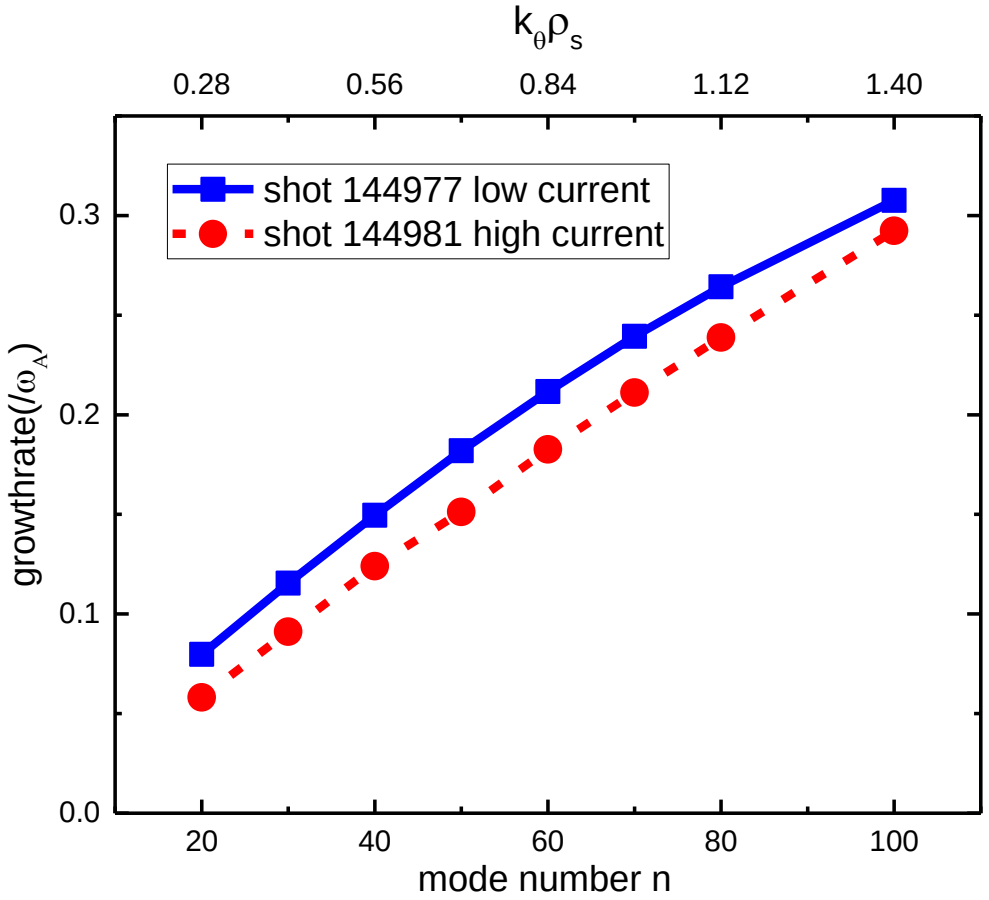

- **The GLF simulations show reliable mode structures**
- **The DIII-D magnetic and plasma profiles are ideal P-B mode stable**
- **The mode is at the outside midplane side, driven by the bad curvature**
- **The Landau damping and toroidal closures are turned off in these initial simulations**

The Landau damping closures have similar impact on the ELM size as flux-limited heat flux

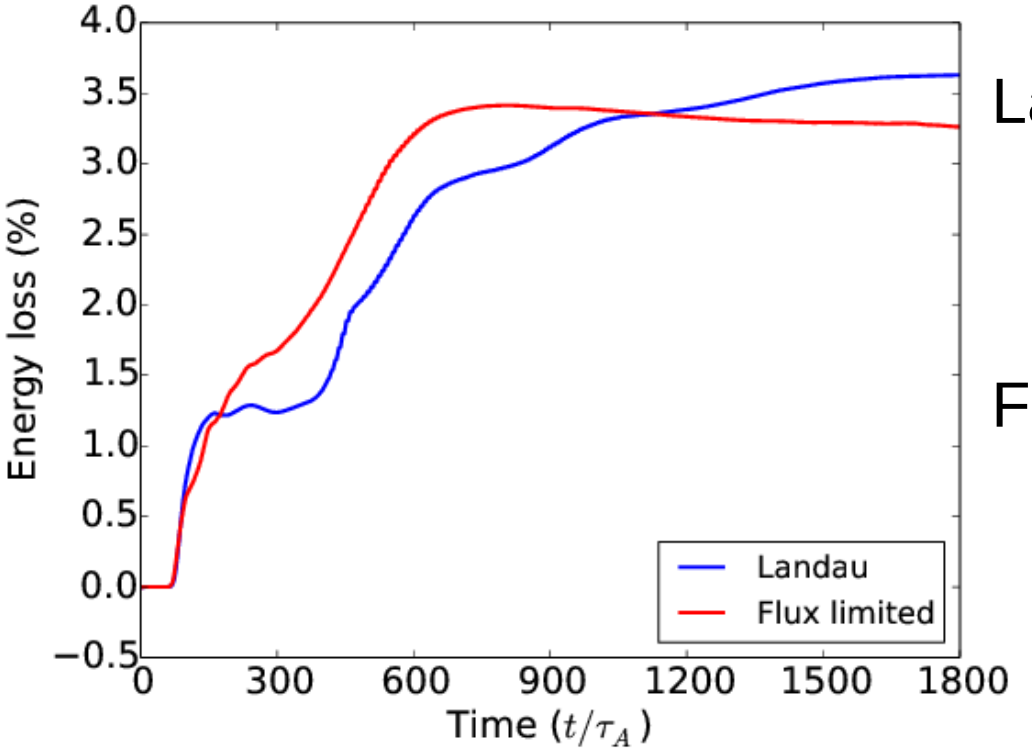

Landau damping:

$$q_{\parallel j} = -n_0 \sqrt{\frac{8}{\pi}} v_{T_j} \frac{i k_\parallel k_B T_j}{|k_\parallel| + \frac{0.5}{\lambda_j}}, j = i, e$$

Flux limiting:

$$q_{\parallel j} = \frac{\kappa_{SH} \kappa_{FS}}{\kappa_{SH} + \kappa_{FS}} \nabla_{\parallel 0} T_j$$

- Nonlinear simulation shows that the energy loss of am ELM are similar with Landau damping closure or flux-limited heat flux in 6-field Landau-fluid simulations.

1. C.H. Ma, X.Q. Xu, *et al.*, *PoP* (2015)

Outline

- Introduction
- Code structure
  - Normalization
  - Implementation
  - Inputs
- Applications
  - Benchmarks
  - Physics results
- Summary

Summary

- The 3+1 GLF model is implemented in the BOUT++ framework for pedestal turbulence and transport;
- The 3+1 GLF model is well benchmarked with other gyrokinetic, gyrofluid and two-fluid codes in both electromagnetic and electrostatic regimes;
- The energy loss of an ELM increases with beta near the first stable region;
- The second stable region of ballooning mode is found in our self-consistent beta scan with the global equilibrium.

Install the 3+1 module

- Get the bout_glf git repository:

```
git clone ssh://user@portal-auth.nersc.gov/project/projectdirs/bout_glf/www/git/bout_glf.git
```

- Switch to the modomegad branch:

```
git checkout bout_modomegad
```

- Compile the code (on cori):

```
./configure --with-netcdf=/global/u2/c/chma/cori/local --with-fftw=/global/u2/c/chma/cori/local
make
cd examples/glfkbm3-1
make
```

Running example

- Launch the linear run job:

```
qsub bout_cori_debug.sh
```

- Get the linear growth rate:

```
python growthrate.py -v -f P data
```

- Example output:

```
Growth rate from linear fit from -20 to -1 is: 0.1491077
```